Topological Characterization of Haze Episodes Using Persistent Homology

Nur Fariha Syaqina Zulkepli[1*], Mohd Salmi Md Noorani[1], Fatimah Abdul Razak[1], Munira Ismail[1] and Mohd Almie Alias[1]

[1] *School of Mathematical Sciences, Faculty of Science and Technology, Universiti Kebangsaan Malaysia 43600 Bangi, Selangor, Malaysia.*

Abstract

Haze phenomenon is one of the major environmental issues that have continuously vexed countries worldwide, including Malaysia, for the last three decades. Therefore, this study aims to investigate the differences between topological features of months with and without haze episodes at air quality monitoring stations located in the areas of Jerantut, Klang, Petaling Jaya, and Shah Alam. This is achieved by opting for persistent homology, which is a method in topological data analysis (TDA) that analyses data in a qualitative (topological) sense via a focus on topological features, such as connected components and holes of the data. Topological features from particulate matter (PM_{10}) data with summary statistics are subsequently utilized to summarize them. The results have consequently shown drastic changes present in the summary statistics of the lifetimes of topological features during haze episodes. These characteristics have been consistently observed in each air quality monitoring station involved in this study. Thus, this finding highlights the potential application for the development of an early warning system for haze detection based on the topological approach.

Keywords: Haze; Particulate matter; Persistent homology; Time delay embedding; Topological data analysis.

[*] Corresponding author. Tel: *+6012-543-2006*

E-*mail address*: farihasyaqina@yahoo.com

INTRODUCTION

Haze phenomenon is one of the major environmental issues that occur continuously in countries across the world; Malaysia included (Wen *et al.*, 2016). The country is also afflicted, with the Klang Valley region being one of the areas that are particularly affected by such phenomenon (Latif *et al.*, 2018). The severity of this issue can be attributed to the large-scale forest and plantation fires that occur in Indonesia's Sumatra Island. Nevertheless, it is worsened further by local emissions from domestic industries, vehicle usage, and open burning activities (Afroz *et al.*, 2003; Wen *et al.*, 2016). In Malaysia, the chronological history of haze episodes can be underlined with the severe incidents recorded in the year 2005, 2013, 2014 and 2015 accordingly (DOE, 2018a). This issue has continually emerged year after year in Malaysia and the neighboring countries of Brunei and Singapore, whereby the prolonged duration of the problem has spurred the study into investigating haze episodes.

Particulate matter (PM_{10}) are small particles floating around in the air in the form of smoke, dirt, and dust that originate from factories, vehicles and farming activities (Schwartz *et al.*, 1996; Payus *et al.*, 2013). During haze episodes, PM_{10} is typically highlighted as a major air pollutant in the Southeast Asian regions, particularly the Klang Valley, Malaysia (Afroz *et al*., 2003; Azmi *et al.*, 2010). Acknowledged as a harmful pollutant, inhalation of the material leads to diminishing lung function and causes various respiratory diseases, especially acute exacerbation of asthma (Schwartz *et al.*, 1996). According to the Malaysian Ambient Air Quality Guidelines

50 (MAAQG), an average of PM_{10} concentration over 24-hour that exceeds 150 $\mu g\, m^{-3}$ is
51 considered to be unhealthy for human health. Therefore, a standard technique used to identify
52 haze phenomenon is by observing the concentration of PM_{10}, whereby haze emergency is
53 declared when it reaches the emergency level (> 500 $\mu g\, m^{-3}$) (DOE, 2018b).

54 Several studies have explored into a comparison of PM_{10} concentration with MAAQG
55 standards, undertaken by Azmi *et al.* (2010), Abdullah *et al.* (2012), Rahman *et al.* (2015) and
56 Ling *et al.* (2010) respectively. They have consequently concluded that the concentration in the
57 air quality monitoring stations located in Klang Valley exceeded the acceptable level
58 recommended by the MAAQG during haze episodes. Various differences have also been revealed
59 between the concentration of PM_{10} according to the locations of air quality monitoring stations,
60 encompassing rural, urban and industrial areas respectively. Moreover, Azmi *et al.* (2010) and
61 Abdullah *et al.* (2012) have also revealed that urban areas logged higher PM_{10} concentration
62 compared to rural areas. A study by Yusof *et al.* (2010) has provided further analysis using a
63 statistical model, Lognormal and Weibull distributions to investigate the relationship between
64 PM_{10} concentration and monsoon season. Similarly, other methods like chemometric analysis
65 (Azid *et al.*, 2015), fuzzy comprehensive evaluation method (Zhao *et al.*, 2010) and chaotic
66 approach (Hamid and Noorani, 2014) have also been utilized in assessing data on air pollutants.
67 Furthermore, haze detection can also be found to be fast gaining scholarly traction. Previously,

works focusing on the topic are geared towards analyzing satellite imagery data using remote sensing methods (Makarau, 2014). Meanwhile, recent research is specifically related to haze periods and focused on analyzing particulate matter concentration to study its morphology during haze episodes (Zeb *et al.*, 2018). Yu *et al.* (2018) have also contributed by investigating human health risk in an indoor and outdoor environment that is exposed to the phenomenon, whereas another study has looked into mitigating severe urban haze episodes (Sharma and Balasubramanian, 2018). It should be noted that these literature has analyzed PM_{10} in a quantitative manner, whereas to the best of our knowledge, no effort has been expended on its qualitative aspects. Therefore, this paper is addressing the research gap by providing an analysis of the qualitative aspects and structures of PM_{10}, particularly on their topological features via persistent homology.

Persistent homology is a relatively new method that is robust under perturbations of input data, independent of coordinates and dimensions alike, and offers a solid representation of qualitative features of the input data (Otter *et al.*, 2017). These particular features of the data are captured accordingly as specific parameters change. As the approach is fundamentally based on the mathematical field of topology, the qualitative features in question encompass topological features like connected components, holes, voids and more. The qualitative approach of persistent homology is also particularly useful in handling complexity of data due to noise, high

dimensionality or incomplete structure. This poses great challenges to researchers dealing with real world data since data cleaning is required in order to remove the noise and which might result in information lost during the process (Jorquera *et al.*, 2000; Elangasinghe *et al.*, 2014). By contrast, persistent homology retains all information from data. The noise that may occur in multiple scale-levels is filtered out by persistent homology and significant features are captured (Ghrist, 2008). Furthermore, its robustness has led other researchers to explore the method further in various fields, such as Gidea and Katz (2018) effort on the capability of the holes (1-dimensional features) to detect financial crisis in stock market data. Meanwhile, Emrani *et al.* (2014) have investigated wheeze signal detection via the persistency of topological features between wheeze and non-wheeze signals. Moreover, the summary statistics of topological features undertaken by Mittal and Gupta (2017) has shown that persistent homology is usable in early detection of bifurcations and chaos in complex system. The explorations on persistent homology have also been tackled in various fields, encompassing the classification of breast cancer (Dewoskin *et al.*, 2010), viral evolution (Chan *et al.*, 2013) and protein structure (Gameiro *et al.*, 2015). A good and comprehensive review regarding the current applications of persistent homology may be sourced from Otter *et al.* (2017). To the best of our knowledge, there is a negligible amount of research output on environmental issues by persistent homology to date. Therefore, this study is conducted to fill the research gap by exploring the effectiveness of

104 persistent homology in characterizing and detecting one of the pressing environmental issues,
105 namely haze phenomenon.

106 This paper intends to investigate haze episodes using persistent homology by analyzing
107 the topological features of PM_{10} data in Malaysia. The proposed technique has been applied to
108 daily average PM_{10} data from four air quality monitoring stations of Jerantut, Klang, Petaling
109 Jaya and Shah Alam from the year 2000 until 2015. The objective of this study is to investigate
110 topological features for months with and without haze episodes, thus rendering the data on PM_{10}
111 being partitioned according to the respective month. The topological features are then extracted
112 for connected components (0-dimensional features) and holes (1-dimensional features), with the
113 resulting information represented in persistence diagrams. Next, the summary statistics of the
114 topological features, like an average of all lifetimes of the connected components and maximum
115 lifetimes of all holes, are calculated for each persistence diagram. In this paper, the content has
116 been organized accordingly, whereby the subsequent section consists of a discussion on data
117 involved in this study. Then, the data transformation processes and the method of persistent
118 homology will be explained in next two sections. Extensive summary statistics of topological
119 features would be introduced in the section before its resulting outcomes is discussed.

120

121

122

DATA

The daily average data for PM_{10} encompassing the year 2000 to 2015 for four air quality monitoring stations (i.e. Jerantut, Klang, Petaling Jaya, and Shah Alam) has been obtained from the Department of Environment (DOE), Malaysia. Klang and Shah Alam are categorized as urban areas, while Petaling Jaya and Jerantut are categorized as respectively of the industrial and rural areas, accordingly (DOE, 2018c). Due to its rural location, Jerantut, in particular, has been chosen as the background station for comparative purpose (Azmi *et al.*, 2010; Banan *et al.*, 2013). Missing data has been treated with the mean substitution method (Pigott, 2001), whereas the MAAQG standards are necessary to represent the safety level that causes no adverse health effects to human. Therefore, this study has adhered to the safe level as recommended by MAAQG to act as the benchmark for air quality level of each station.

Fig. 1 shows the time series of the daily average for PM_{10} from 1 January 2000 until 31 December 2015, and the MAAQG for a 24-hour average PM_{10} at 150 $\mu g\ m^{-3}$. The presence of several peaks (rectangles) is indicative of the values of PM_{10} concentration exceeding the MAAQG during haze episodes that have occurred in August 2005, June 2013, March 2014, September 2015, and October 2015 accordingly (DOE, 2018a). Thus, these months have been highlighted as the main focus of this research. It is worth noting that based on the chronology of haze episodes (DOE, 2018a), the selected months have been reported of experiencing severe haze.

142 The descriptive statistics of the months are shown in Table 1 accordingly, with Klang, Petaling
143 Jaya and Shah Alam stations showing higher concentration of PM_{10} compared to Jerantut station
144 during the haze episodes. This is attributable to the different locations of the air quality
145 monitoring stations, with Klang and Shah Alam being located in an urban area, Petaling Jaya in
146 an industrial area and Jerantut (background station) in a rural area (DOE, 2018c).
147
148 **TIME DELAY EMBEDDING**
149
150 Prior to the implementation of persistent homology, the time series data sets must be
151 transformed into point cloud data, which is achieved via the Takens method. The higher
152 dimensional data sets will allow us to look into higher dimensional topological features, such as
153 holes and voids. Basically topological features are features that are invariant after deformations
154 such as stretching, splitting and cutting (Hatcher, 2002; Edelsbrunner and Harer, 2010; Ghrist,
155 2014). The idea of using a combination of Takens method and persistent homology is discussed
156 in the work of Perea and Harer (2015) and references therein. The Takens method (Takens, 1981)
157 stated that a time series $x_0, x_1, ..., x_{n-1}$ can be reconstructed in a phase space of dimension m,
158 where each point in the phase space is given by the vector $x_n(m,\tau) = x_n, x_{n+\tau}, ..., x_{n+(m-1)\tau}, \tau$ is
159 the time delay and m is the embedding dimension. The two parameters τ and m require careful
160 selection to ensure clear extraction of the desired topological features. In this study, a comparison
161 made between the months has indicated that the different settings of time delay and embedding

dimension will affect the results. The two parameters have been fixed as $\tau = 1$ and $m = 3$. The time delay is chosen as trivial time delay, whereas the embedding dimension chosen is 3 as the 1-dimensional topological features are best visualized in dimension 3 throughout the study. This decision is supported by Umeda (2017), whose work has fixed both parameters as $\tau = 1$ and $m = 3$, while others like Khasawneh *et al.* (2018) and Khasawneh and Munch (2014) chose $m = 3$ to visualize the 1-dimensional features. Similarly, previous studies by Pereira and Mello (2015) and Maletić *et al.* (2016) have also fixed m, whereas in other areas of research (not related to persistent homology), Sivakumar (2003) and Sivakumar (2002) each have chosen $\tau = 1$ to achieve better results for their respective research.

PERSISTENT HOMOLOGY

Computations of simplicial complexes are compulsory in extracting topological features from point clouds data. The 0-simplices represent vertices or points, 1-simplices represent edges or lines, 2-simplices represent triangles and 3-simplices represent tetrahedra, and so on. A simplicial complex is built by a combination of these simplices (See Fig. 2) accordingly, whereby its complex formation is from data points and thus indicating the dependency of topological features on a scaling parameter (filtration value), ε. Fig. 3(a) in particular shows an example of a simplicial complex formation. The formation commenced at $\varepsilon = 0$, where the four 0-simplices formed represents four points in a point cloud. As the value ε increases to 0.5, four circles are

formed with each 0-simplex acting as the centre and ε as the radius of the circles. The circles keep growing as the value ε increases until any pair of the circles intersects each other. From this intersection, a 1-simplex is formed by connecting two 0-simplices by a line (edge). As seen in Fig. 3(a), four 1-simplices have been formed at $\varepsilon = 1.4$, and the stage is marked with the formation of a simplicial complex via the combination of the 0-simplices and 1-simplices. The ε value then further increased to 2, with more circles intersecting each other and resulting in the appearance of two 2-simplices (triangles). At this stage, a new simplicial complex is formed (see Fig. 3(a)). It should be noted that the simplicial complex at $\varepsilon = 1.4$ is contained in the simplicial complex at $\varepsilon = 2$, which is also known as filtered simplicial complexes. In this work, the constructions of simplicial complexes are done using Vietoris-Rips simplicial complex, or otherwise also known as Rips complex. Rips complex is a set of *k*-simplices, such that the distance of any two points in *k*-simplices is less than or equal to 2ε (Hatcher, 2002; Edelsbrunner and Harer, 2010; Ghrist, 2014).

The birth and death points of topological features are captured depending on the formation of simplicial complexes and subsequently recorded in a diagram known as barcode (Fig. 3(b)). Each feature is represented by a horizontal line in the barcode, with the left end point of the line being the birth point and the right end point of the line considered as the death point. One can recognize any noise in the barcode by looking at the short lines, while the significant

features are signified by the long lines (Ghrist, 2008). Furthermore, the black lines in the barcode represent the connected components, whereas the red line represents the hole (see Fig. 3(b)). Moreover, persistence diagram (Fig. 3(c)) is yet another representation of barcode that serves to summarize the birth and death of topological features in $\mathbb{R}^2$. The *x*-axis and *y*-axis of the persistence diagram is the representation of the birth and death points respectively for each of the topological features. Besides, a point (b,d) with multiplicity q in a persistence diagram represents q features that have same birth, b and death, d points. Another feature that persists longer through the filtration stage is located way above the diagonal line in the persistence diagram. Additionally, the persistency of a feature is measured by the difference between the death and birth points, $d-b$ and subsequently known as the lifetime of the feature (Otter *et al*., 2017).

Fig. 3 shows an example of connected components (0-dimensional) and hole (1-dimensional) extracted based on the formation of simplicial complexes. At the starting point, four connected components have appeared with a birth value at $\varepsilon = 0$, and as the filtration value increases the features have remained until 1-simplices appeared at $\varepsilon = 1.4$. It should be noted that the four connected components have collapsed into one at $\varepsilon = 1.4$. Interestingly, a new feature has appeared at this stage, represented by a hole appearance. As the values of ε have continued to increase to 2, two 2-simplices are subsequently formed and closed the hole. This causes the

death of the hole and renders only one connected component to persist by the end of the filtration. Persistence diagram in Fig. 3(c) is another representation of these topological features, simplifying the barcode in Fig. 3(b).

SUMMARY STATISTICS OF TOPOLOGICAL FEATURES

A persistence diagram consists of *k*-dimensional features with 0-dimensional features representing the connected components, 1-dimensional features representing holes, and 2-dimensional features representing voids etc. Meanwhile, a persistence diagram ω_m consists of n features $\omega_{m_i} = (b_i, d_i)$ with b_i and d_i $(i = 1,2,...,n)$ indicating their birth and death points respectively. All of the features are summarized using summary statistics and described below:

The first summary statistic is the sum of all lifetimes (Eq. (1)) (Pereira and Mello, 2015) of *k*-dimensional features. If the value of the sum is close to zero, the persistence diagram has practically short-lived features for each particular dimension, *k*.

$$\text{sum}_k = \sum_{i=1}^{n} (d_i - b_i). \quad (1)$$

The second summary statistic is the average of all lifetimes (Pereira and Mello, 2015; Mittal and Gupta, 2017) of *k*-dimensional features, as described in Eq. (2). Likewise, a small value of average indicates that for a particular dimension, *k* of the data set has mostly short-lived features and vice versa.

$$\mathrm{avg}_k = \frac{\sum_{i=1}^{n}(d_i - b_i)}{n}. \quad (2)$$

Next, the third summary statistic is the maximum of all lifetimes (Pereira and Mello, 2015; Mittal and Gupta, 2017) of k-dimensional features. For each dimension k, the value of the maximum lifetimes of all features is defined as

$$\max_k = \max_{\omega_{m_i}} (d_i - b_i), \quad (3)$$

which will determine the most significant k-dimensional feature.

In this study, the summary statistics of 0-dimensional and 1-dimensional features have been calculated using Eqs. (1-3). The changes of values in each summary statistics have been observed to track the evolution of the topological features for months with and without haze accordingly.

Remark. We acknowledge that according to Cohen-Steiner *et al.* (2007) and Cohen-Steiner *et al.* (2010), the summary statistic, sum_k is stable whereas the stability of the avg_k is still in doubt. However, there may be merit in taking into account avg_k as considered by Pereira and Mello (2015) and Mittal and Gupta (2017) but in general it should be done with care. Based on our observations using our data sets, small variation of the input data leads to small variation of avg_k values.

RESULTS

This study has analyzed the time series of daily average for PM_{10} that is partitioned according to month for four air quality monitoring stations located in Jerantut, Klang, Petaling Jaya, and Shah Alam for 16 years (2000-2015). The time delay embedding with time delay $\tau = 1$ and embedding dimension $m = 3$ have been applied for each month of data on PM_{10}, allowing each month to generate a point cloud data. Persistent homology is then applied to each point cloud with maximum filtration value, $\varepsilon_{\max} = 700$. The evolution of topological features based on Rips complexes is next observed in the range of filtration value, $\varepsilon = [0, 700]$, starting from the simplest form which is under-approximation until it displays over-estimation (i.e. one large Rips complex). The computation of persistent homology in this study has been completed using the R-package TDA (Fasy *et al.*, 2017).

All extracted topological features have been represented in persistence diagrams, following which the summary statistics for each persistence diagrams have been calculated. Fig. 4 has displayed a comparison between persistence diagrams generated in August 2005 where severe haze has been reported (DOE, 2018a), in contrast with December 2005 where no haze has occurred. The point clouds generated using time delay embedding which respect to the persistence diagrams are also shown in Fig. 4. The month of December has been selected due to the lesser likelihood for haze to occur during the north-east monsoon (November to March)

season, as Malaysia receives more rainfall during the period and increases the removal rate of PM_{10} (Yusof *et al.*, 2010).

From the persistence diagrams shown in Fig. 4, the topological features (i.e. black dots represent connected components, red triangles represent holes) for a month with haze episode recorded (i.e. August 2005) is spread away from the origin. In contrast, a month without haze (i.e. December 2005) has shown that the features accumulate close to the origin. For each station, a hole is present among the holes (red triangles) as in Fig. 4(a), which is located the furthest from the origin and the highest value of birth and death points compared to other holes. It should be noted the corresponding feature in Jerantut is not too far from the origin compared to other stations, implying that the stations in Klang, Shah Alam, and Petaling Jaya have experienced haze of higher severity compared to Jerantut. Summary statistics are calculated to summarize the persistence diagrams, whereby the resulting outcomes are shown in Fig. 5 and Fig. 6.

An observation of the various peaks in Fig. 5(a) has revealed drastic increments of the sum of all lifetimes, sum_0 for connected components (0-dimensional features) during haze episodes (rectangles). This is indicative of the connected components persisting longer during haze as the filtration value varied compared to the normal months. This is further elucidated by the average of all lifetimes, avg_0 as shown in Fig. 5(b), which suggests that the persistence diagrams for months with haze consist of mostly long-lived features, hence producing the peaks.

Fig. 5(a) and 5(b) also show that the sum and average of the lifetimes of connected components extracted in the background station, Jerantut being the lowest compared to other stations. It should be noted that the maximum of all lifetimes are not calculated for connected components as the formation of simplicial complexes (Rips complexes) for PM_{10} persists until it becomes a large simplicial complex with birth, $b = 0$ and death, $d = 700$ (since maximum filtration value, $\varepsilon_{\max} = 700$) resulting in the same values of maximum for all lifetimes ($\max_0 = 700$) according to all selected months.

Furthermore, the summary statistics for holes (1-dimensional features) are shown in Fig. 6 and revealed drastic changes in the values of the sum, average and maximum of all lifetimes denoted as $\text{sum}_1, \text{avg}_1$ and $\max_1$ respectively (refer Fig. 6(a-c)) during haze episodes (rectangles). As seen in Fig. 6(c), the peaks (in rectangles) are the values of a maximum of the lifetimes of all holes which imply that there is a hole with its lifetime higher compared to other holes in the month that experienced severe haze. Hence, Fig. 5 and Fig. 6 have revealed the behavior of the topological features extracted by persistent homology to be consistent with real haze phenomenon. When the haze occurred, persistent homology has identified this occurrence by showing the strong rise of the lifetimes for related topological features.

The rectangles in Fig. 5 and Fig. 6 indicate the particular month recorded with severe haze in the selected years, with a clear and drastic increase in the values of summary statistics in the

311 month. These characteristics have also been shown by each station involved, substantiating the
312 consistency of the topological characterization for months with and without haze accordingly.
313 Overall, the values (i.e. summation, average, maximum) of all lifetimes for the topological
314 features of the background station (Jerantut) are the lowest compared with the others. Thus, it is
315 clear that the topological features extracted via persistent homology are capable of distinguishing
316 the months with severe haze and without haze. While the existing methods (Azmi *et al.*, 2010;
317 Ling *et al.*, 2010; Abdullah *et al.*, 2012; Rahman *et al.*, 2015) have served to directly quantify
318 PM_{10} concentration without providing a qualitative understanding, this paper has successfully
319 filled in research gap by revealing the changes of topological features seen between months with
320 and without haze accordingly.
321
322 **CONCLUSIONS**
323
324 This study has opted for the method from topological data analysis (TDA) known as
325 persistent homology so as to qualitatively analyze the topological features embedded within the
326 data on the concentration of a major pollutant, PM_{10}. The changes of topological features have
327 been found in the months that recorded severe haze episodes, which have been consistently
328 shown in each station involved in this study. Despite existing methods is capable of quantifying
329 and analyzing the concentration of PM_{10} directly in determining the months affected during haze
330 episodes, this study has proposed a different approach for analysis based on the topological

viewpoint. The topological characterization of haze episodes complement the existing methods by providing its qualitative structures which is robust to the effect of noise. The summary statistics of the topological features (i.e. connected components and holes) have indicated a strong rising of the sum, average and maximum of all lifetimes of the topological features during haze episodes. Furthermore, topological features PM_{10} extracted from different locations of air quality monitoring stations have succeeded in characterizing Jerantut as the background station to have a low level of air pollution. This is seen by the lowest values of summary statistics compared to other stations (i.e. Klang, Petaling Jaya, and Shah Alam). Thus, this study proposed a new approach to analyze haze episodes using a qualitative approach, specifically by extracting topological features that can characterize haze episodes. This is done by observing the summary statistics of such topological features. Hence, this finding has displayed its potential as an application for the development of an early warning system for haze detection, based on the topological approach. We particularly believe that early warning signals can be determined by refining the way data is analyzed and the progressive efforts spearheaded by this work is making waves in the particular area. We also suggest future research in addressing the stability of summary statistic, avg_k since the referee has pointed out that it's stability is still unknown.

ACKNOWLEDGMENTS

The authors would like to express their utmost gratitude to Universiti Kebangsaan Malaysia for the Research University Grant (DIP-2017-011, GGPM-2016-001), Ministry of Education Malaysia Grant FRGS/1/2017/STG06/UKM/01/1, and to Department of the Environment (DOE) for providing the air quality data. We also thank the reviewers for their helpful and critical comments.

370 **REFERENCES**

371

372 Abdullah, A.M., Samah, M.A.A. and Jun, T.Y. (2012). An overview of the air pollution trend in
373 Klang Valley, Malaysia. *Open Environmental Sciences*. 6(1): 13–19.

374 Afroz, R., Hassan, M.N. and Ibrahim, N.A. (2003). Review of air pollution and health impacts in
375 Malaysia. *Environ. Res.* 92(2): 71–77.

376 Azid, A., Juahir, H., Ezani, E., Toriman, M.E., Endut, A., Rahman, M.N.A., Yunus, K., Nordin,
377 M., Kamarudin, M.K.A., Hasnam, C.N.C., Saudi, A.S.M. and Umar, R. (2015). Identification
378 source of variation on regional impact of air quality pattern using chemometric. *Aerosol Air*
379 *Qual. Res*. 15: 1545–1558.

380 Azmi, S.Z., Latif, M.T., Ismail, A.S., Juneng, L. and Jemain, A.A. (2010). Trend and status of air
381 quality at three different monitoring stations in the Klang Valley, Malaysia. *Air Qual. Atmos.*
382 *Health*. 3(1): 53–64.

383 Banan, N., Latif, M.T., Juneng, L. and Ahamad, F. (2013). Characteristics of surface ozone
384 concentrations at stations with different backgrounds in the Malaysian Peninsula. *Aerosol Air*
385 *Qual. Res*. 13(3): 1090-1106.

386 Chan, J.M., Carlsson, G. and Rabadan, R. (2013). Topology of viral evolution. Proceedings of the
387 National Academy of Sciences. 110(46): 18566–18571.

388 Cohen-Steiner, D., Edelsbrunner, H., and Harer, J. (2007). Stability of persistence

389 diagrams. *Discrete Comput. Geom.* 37(1): 103-120.

390 Cohen-Steiner, D., Edelsbrunner, H., Harer, J. and Mileyko, Y. (2010). Lipschitz functions have

391 L_p-stable persistence. *Found. Comput. Math.* 10(2): 127-139.

392 Dewoskin, D., Climent, J., Cruz-White, I., Vazquez, M., Park, C. and Arsuaga J. (2010).

393 Applications of computational homology to the analysis of treatment response in breast cancer

394 patients. *Topol. Appl*. 157(1): 157–164.

395 DOE (2018a). Chronology of haze episodes in Malaysia. Department Of Environment Malaysia.

396 https://www.doe.gov.my/portalv1/en/info-umum/info-kualiti-udara/kronologi-episod-jerebu-

397 di-malaysia/319123. Last Access: 10 July 2018.

398 DOE (2018b). A guide to air pollutant index (API) in Malaysia. Department Of Environment

399 Malaysia. Enviro Knowledge Centre. https://enviro.doe.gov.my/. Last Access: 10 August 2018.

400 DOE (2018c). Environmental quality report 2015. Department Of Environment Malaysia. Enviro

401 Knowledge Centre. https://enviro.doe.gov.my/ . Last Access: 10 July 2018.

402 Edelsbrunner, H. and Harer, J. (2010). *Computational topology: an introduction*. American

403 Mathematical Society, Providence.

404 Elangasinghe, M.A., Singhal, N., Dirks, K.N., and Salmond, J.A. (2014). Development of an

405 ANN–based air pollution forecasting system with explicit knowledge through sensitivity

406 analysis. *Atmospheric pollution research*. *5*(4): 696-708.

407 Emrani, S., Gentimis, T. and Krim, H. (2014). Persistent homology of delay embeddings and its
408 application to wheeze detection. *IEEE Signal Process. Lett.* 21(4): 459–463.
409 Fasy, B.T., Kim, J., Lecci, F., Maria, C. and Rouvreau, V. (2017). Statistical tools for topological
410 data analysis. arXiv: Mathematical Software: Available from https://cran.r
411 project.org/web/packages/TDA/TDA.pdf.
412 Gameiro, M., Hiraoka, Y., Izumi, S., Kramar, M., Mischaikow, K. and Nanda, V. (2015). A
413 topological measurement of protein compressibility. *Jpn. J. Ind. Appl. Math*. 32(1): 1–17.
414 Ghrist, R. (2008). Barcodes: The persistent topology of data. *Bulletin of the American*
415 *Mathematical Society*. 45(1): 61–75.
416 Ghrist, R.W. (2014). *Elementary applied topology*, Seattle: Createspace.
417 Gidea, M. and Katz, Y.A. (2018). Topological Data Analysis of financial time series: landscapes
418 of crashes. *Physica A: Statistical Mechanics and its Applications*. 491: 820-834.
419 Hamid, N.Z.A. and Noorani, M.S.M. (2014). A pilot study using chaotic approach to determine
420 characteristics and forecasting of PM10 concentration time series. *Sains Malaysiana*. 43(3):
421 475–481.
422 Hatcher, A. (2002). *Algebraic topology*. Cambridge University Press, Cambridge.
423 Jorquera, H., Palma, W., and Tapia, J. (2000). An intervention analysis of air quality data at
424 Santiago, Chile. *Atmos. Environ*. 34(24): 4073-4084.

425 Khasawneh, F.A. and Munch, E. (Eds.) ASME 2014 International Mechanical Engineering
426 Congress and Exposition 2014, American Society of Mechanical Engineers, Montreal, Canada.
427 Khasawneh, F.A., Munch, E. and Perea, J.A. (2018). Chatter Classification in Turning Using
428 Machine Learning and Topological Data Analysis. arXiv:1804.02261 (Preprint).
429 Latif, M.T., Othman, M., Idris, N., Juneng, L., Abdullah, A.M., Hamzah, W.P., Khan, M.F.,
430 Sulaiman, N.M.N., Jewaratnam, J., Aghamohammadi, N., Sahani, M., Chung, J.X., Ahamad,
431 F., Amil, N., Darus, M., Varkkey, H., Tangang, F. and Jaafar, A.B. (2018). Impact of regional
432 haze towards air quality in Malaysia: a review. *Atmos. Environ*. 177: 28-44.
433 Ling, O.H.L., Ting, K.H., Shaharuddin, A., Kadaruddin, A. and Yaakob, M.J. (2010). Urban
434 growth and air quality in Kuala Lumpur city, Malaysia. *Environ. Asia*. 3(2): 123-128.
435 Makarau, A., Richter, R., Muller, R. and Reinartz, P. (2014). Haze detection and removal in
436 remotely sensed multispectral imagery. *IEEE Trans. Geosci. Remote. Sens*. 52(9): 5895–5905.
437 Maletić, S., Zhao, Y. and Rajković, M. (2016). Persistent topological features of dynamical
438 systems. Chaos: *An Interdisciplinary Journal of Nonlinear Science*. 26(5): 053105.
439 Mittal, K. and Gupta, S. (2017). Topological characterization and early detection of bifurcations
440 and chaos in complex systems using persistent homology. *Chaos: An Interdisciplinary Journal*
441 *of Nonlinear Science*. 27(5):051102.
442 Otter, N., Porter, M.A., Tillmann, U., Grindrod, P. and Harrington, H.A. (2017). A roadmap for
443 the computation of persistent homology. *EPJ Data Sci*. 6(1): 17.

444 Payus, C., Abdullah, N. and Sulaiman, N. (2013). Airborne particulate matter and meteorological
445 interactions during the haze period in Malaysia. *International Journal of Environmental*
446 *Science and Development*. 4(4): 398-402.

447 Perea, J.A. and Harer, J. (2015). Sliding windows and persistence: An application of topological
448 methods to signal analysis. *Foundations of Computational Mathematics*. 15(3), 799-838.

449 Pereira, C.M. and Mello, R.F.D. (2015). Persistent homology for time series and spatial data
450 clustering. *Expert Syst Appl*. 42(15-16): 6026–6038.

451 Pigott, T.D. (2001). A review of methods for missing data. *Educ. Res. Eval*. 7(4): 353–383.

452 Rahman, S.R., Ismail, S.N., Ramli, M.F., Latif, M.T., Abidin, E.Z. and Praveena, S.M. (2015).
453 The assessment of ambient air pollution trend in Klang Valley, Malaysia. *World Environment*.
454 5(1): 1-11.

455 Schwartz, J., Dockery, D.W. and Neas, L.M. (1996). Is daily mortality associated specifically
456 with fine particles? *J. Air. Waste. Manag. Assoc.* 46(10): 927–939.

457 Sharma, R. and Balasubramanian, R. (2018). Size-fractionated Particulate Matter in Indoor and
458 Outdoor Environments during the 2015 Haze in Singapore: Potential Human Health Risk
459 Assessment. *Aerosol Air Qual. Res*. 18(4): 904-917

460 Sivakumar, B. (2002). A phase-space reconstruction approach to prediction of suspended
461 sediment concentration in rivers. *J. Hydrol*. 258(1-4): 149-162.

462 Sivakumar, B. (2003). Forecasting monthly streamflow dynamics in the western United States: a

463 nonlinear dynamical approach. *Environ. Modell. Softw.* 18(8-9):721–728.

464 Takens, F. (1981). Detecting strange attractors in turbulence. Lecture Notes in Mathematics
465 Dynamical Systems and Turbulence, Warwick 1980: 366–381.

466 Umeda, Y. (2017). Time series classification via Topological Data Analysis. *Trans. Jpn. Soc.*
467 *Artif. Intell*. 32(3): D-G72_1-12.

468 Wen, Y.S., Mohd Nor, A.F., Fazilan, N.N. and Sulaiman, Z. (2016). Transboundary air pollution
469 in Malaysia: Impact and Perspective on Haze. *Nova Journal of Engineering and Applied*
470 *Sciences*. 5(1): 1–11.

471 Yu, S., Li, P., Wang, L., Wu, Y., Wang, S., Liu, K., Zhu, T., Zhang, Y., Hu, M., Zeng, L., Zhang,
472 X., Cao, J., Alapaty, K., Wong, D.C., Pleim, J., Mathur, R., Rosenfeld, D. and Seinfeld J.H.
473 (2018). Mitigation of severe urban haze pollution by a precision air pollution control approach.
474 *Sci. rep.* 8(1): 8151.

475 Yusof, N.F.F.M., Ramli, N.A., Yahaya, A.S., Sansuddin, N., Ghazali, N.A. and Madhoun, W.A.
476 (2010). Monsoonal differences and probability distribution of PM10 concentration. *Environ.*
477 *Monit. Assess.* 163(1-4): 655–667.

478 Zeb, B., Alam, K., Sorooshian, A., Blaschke, T., Ahmad, I. and Shahid, I. (2018). On the
479 morphology and composition of particulate matter in an urban environment. *Aerosol Air Qual.*
480 *Res*. 18: 1431-1447.

481 Zhao, X., Qi, Q. and Li, R. (2010). The establishment and application of fuzzy comprehensive
482 model with weight based on entropy technology for air quality assessment. *Procedia Eng*. 7:

217–222.

489 **Table 1.** Descriptive statistics for daily average of PM_{10} for the chosen months, August 2005,
490 June 2013, March 2014, September and October 2015.

Month	Statistic	Station			
		Jerantut	**Klang**	**Petaling Jaya**	**Shah Alam**
Aug-05	Min	35	36	43	26
	Max	205	590	482	587
	Mean	76.12903	139.5161	119.2581	114.8064516
	Std. Deviation	47.34888	138.0956	111.0225	135.0062762
Jun-13	Min	19	36	20	21
	Max	211	581	370	362
	Mean	56.56667	122	84.26667	83.23333333
	Std. Deviation	43.06826	125.8639	82.18731	81.23940072
Mar-14	Min	17	47	33	36
	Max	49	448	303	279
	Mean	28.67742	137.9355	94.64516	94.67741935
	Std. Deviation	7.943077	98.63364	65.17134	62.35457059
Sep-15	Min	35	59	49	49
	Max	242	337	295	301
	Mean	101.8333	141.4333	123.2	135.4
	Std. Deviation	52.76629	69.77584	64.72403	66.17458623
Oct-15	Min	13	52	24	42
	Max	176	326	320	346
	Mean	75.64516	158.6774	125.5484	147.4516129
	Std. Deviation	49.42034	76.16972	72.68509	78.30829616

491

492

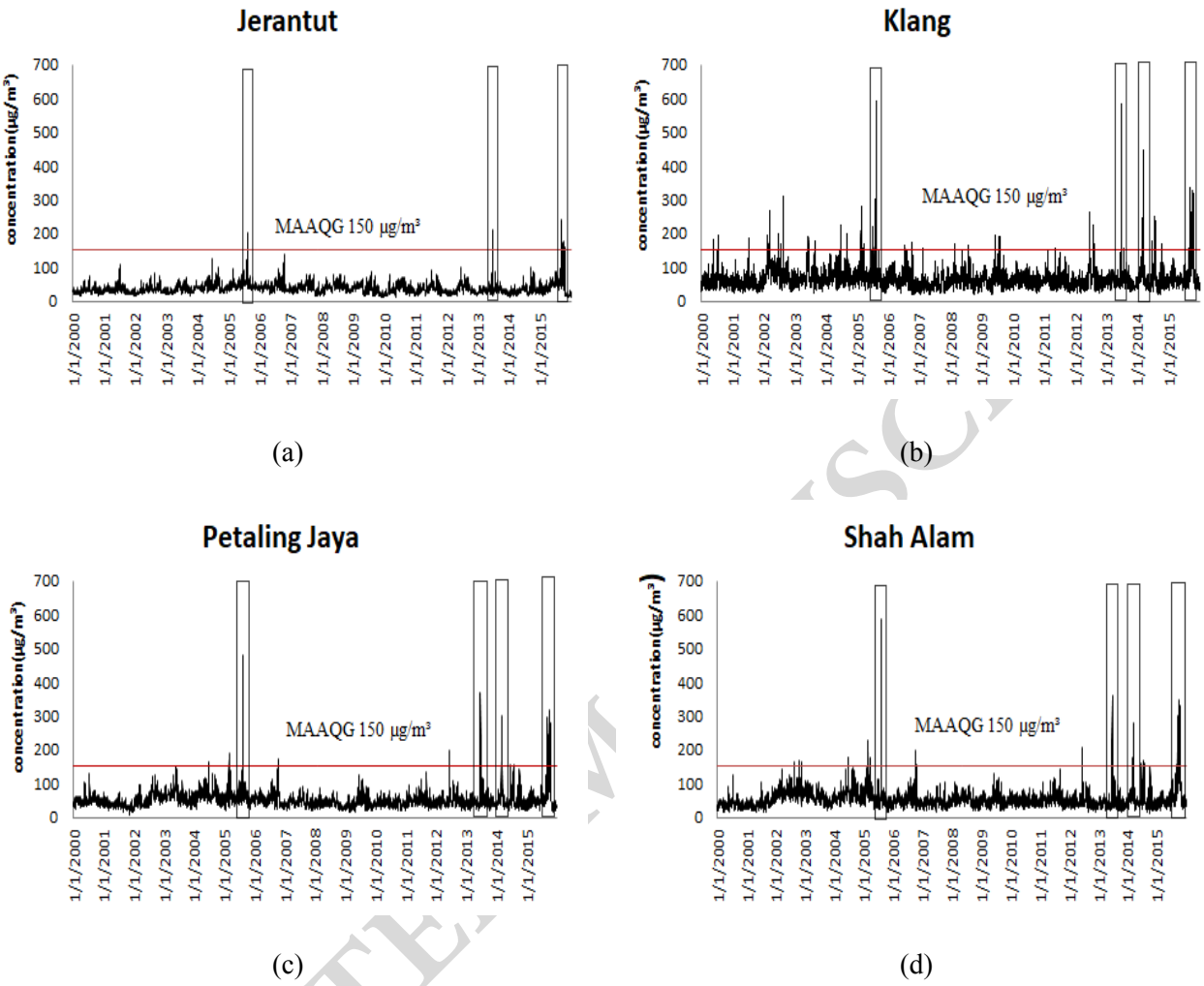

Fig. 1. Time series of daily average of PM_{10} for (a) Jerantut, (b) Klang, (c) Petaling Jaya and (d) Shah Alam air quality monitoring stations from 1 January 2000 until 31 December 2015.

493

494

495

496

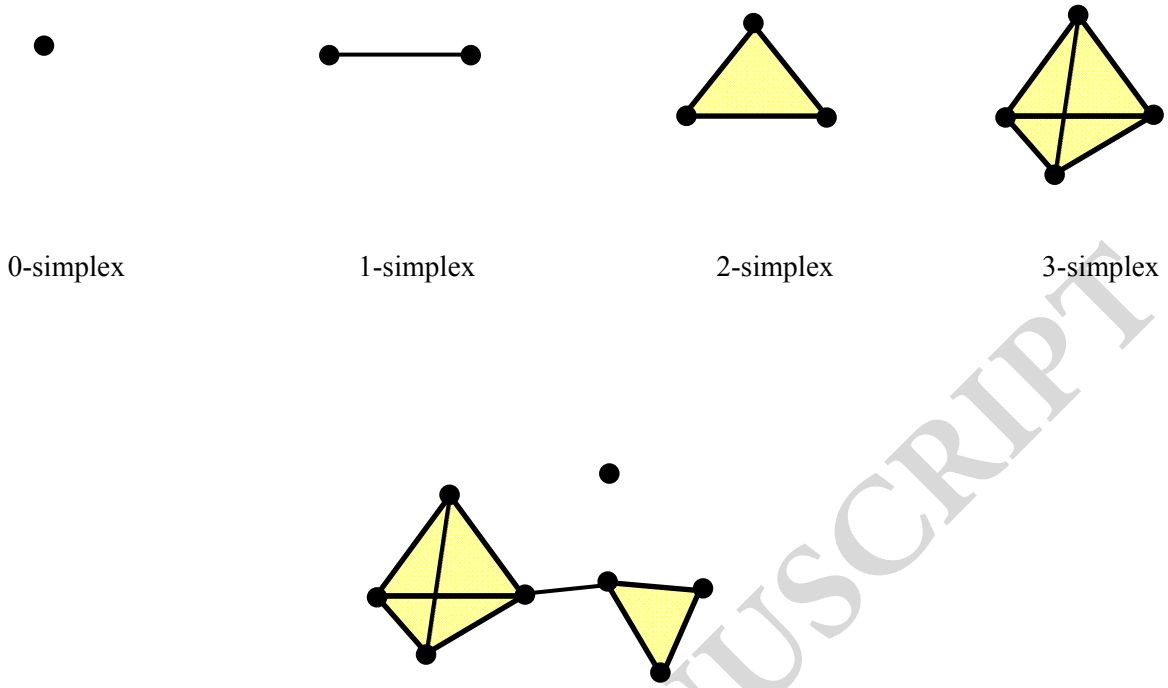

Fig. 2. *k*-simplices for $0 \leq k \leq 3$.

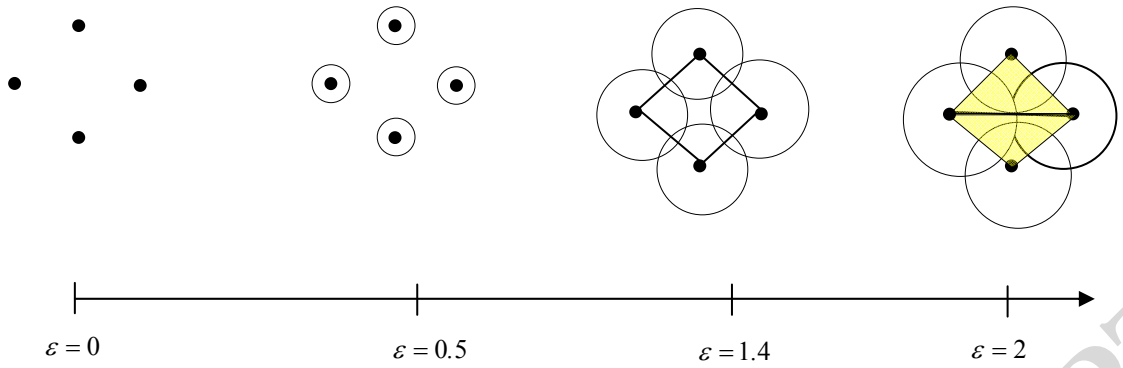

(a)

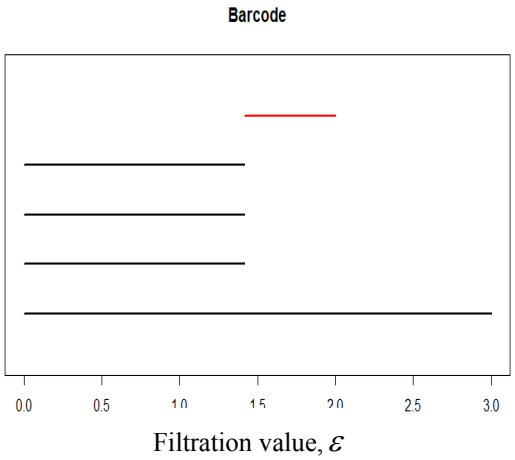

(b)

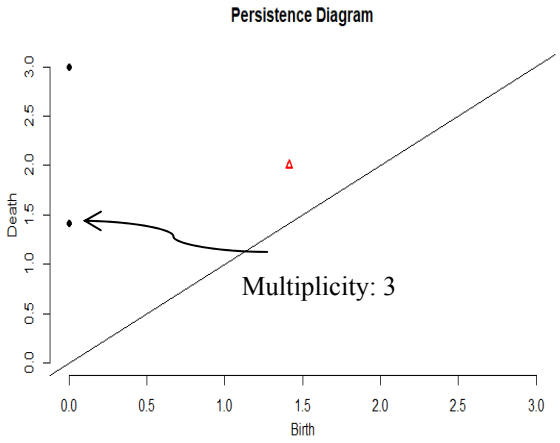

(c)

Fig. 3. (a) Formation of simplicial complexes with respect to the filtration values, ε. (b)(c) Barcode and persistence diagram for the formation of simplicial complex illustrated in (a). In (b) and (c), the black lines and black dots represent connected components in (a), while red line and red triangle correspond to hole in (a).

505

506

507

508

509

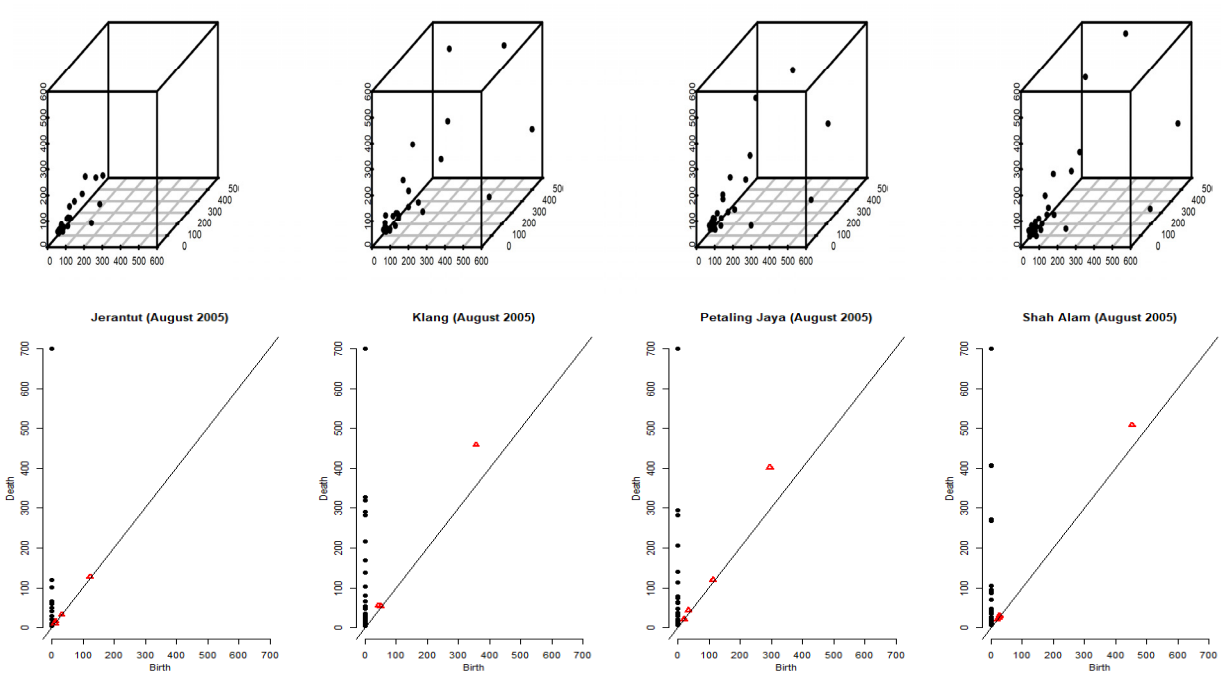

(a)

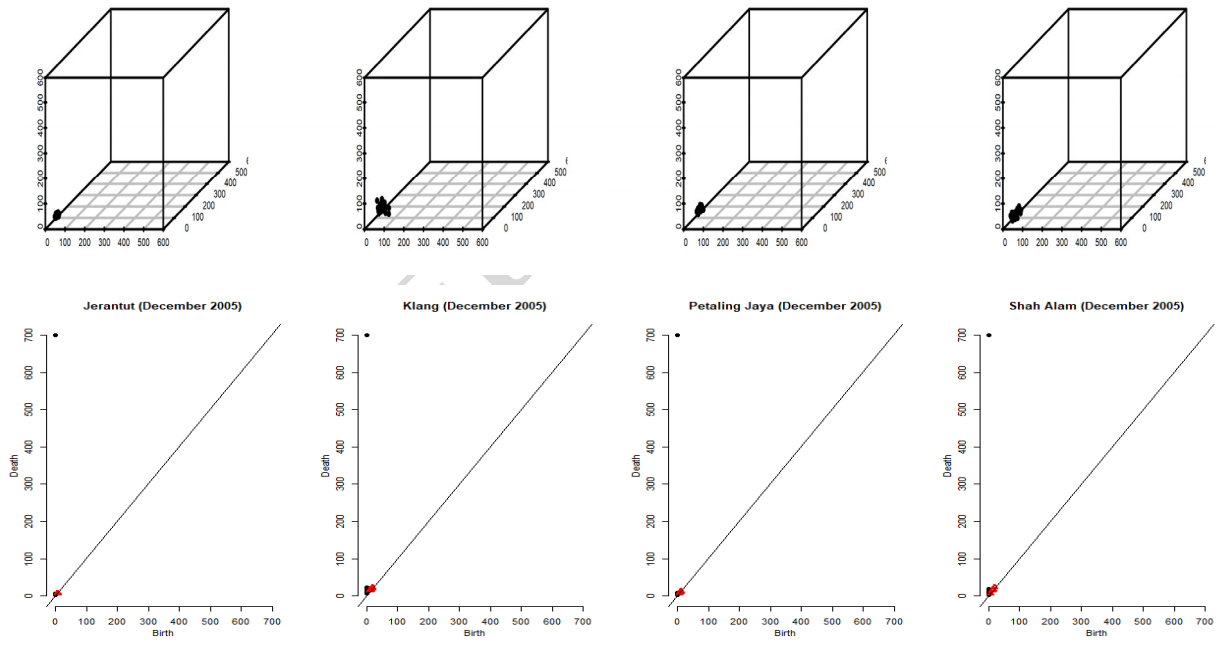

(b)

Fig. 4. Point clouds and persistence diagrams for the months with haze, August 2005 (a) and without haze, December 2005 (b) for Jerantut, Klang, Petaling Jaya and Shah Alam stations (left to right). The black dots and red triangles in persistence diagrams represent connected components and holes.

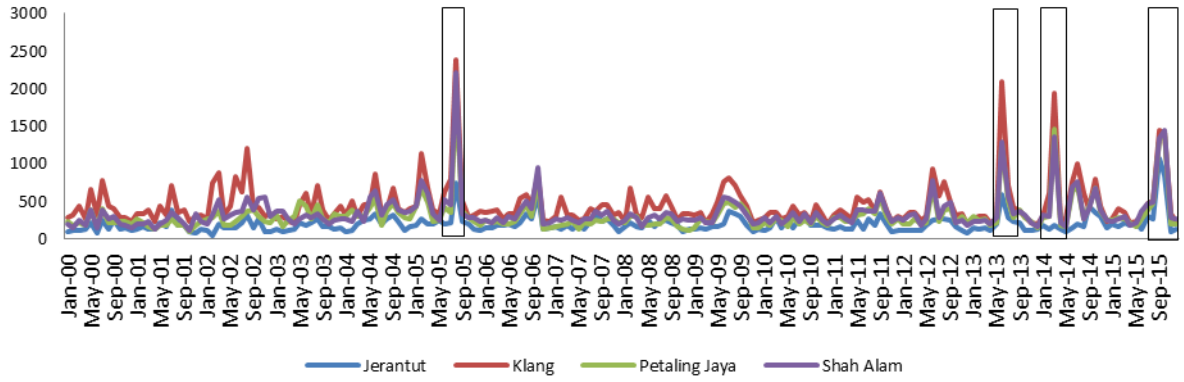

(a)

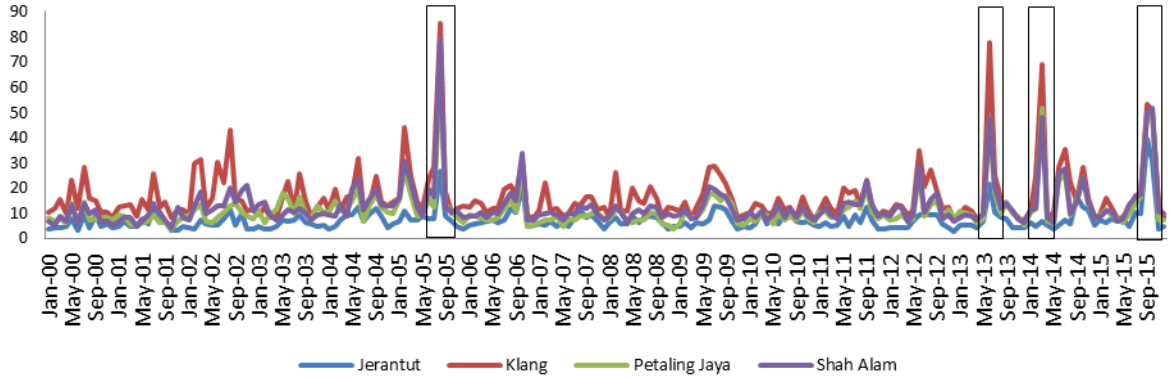

(b)

Fig. 5. (a) sum_0 of all lifetimes and (b) avg_0 of all lifetimes, for four air quality monitoring stations Jerantut, Klang, Petaling Jaya and Shah Alam. The rectangles indicate the months with severe haze episodes namely August 2005, June 2013, March 2014 and September and October 2015 (left to right).

512

513

514

515

516

517

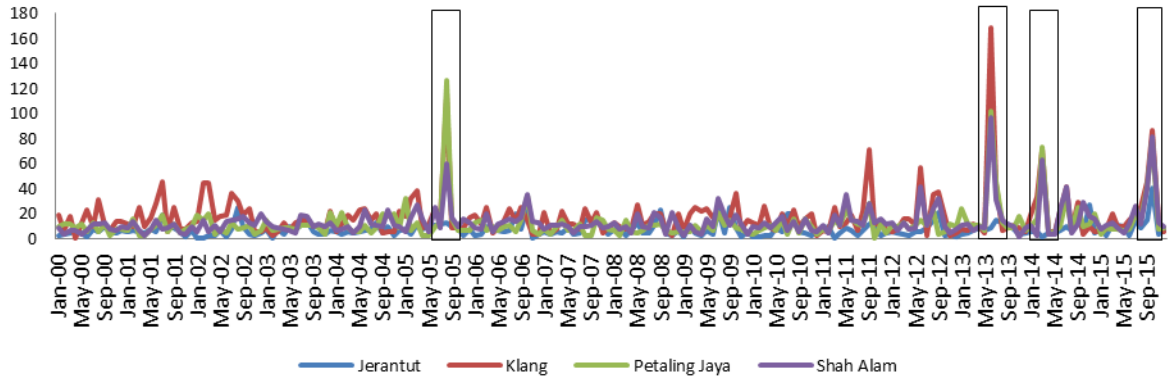

(a)

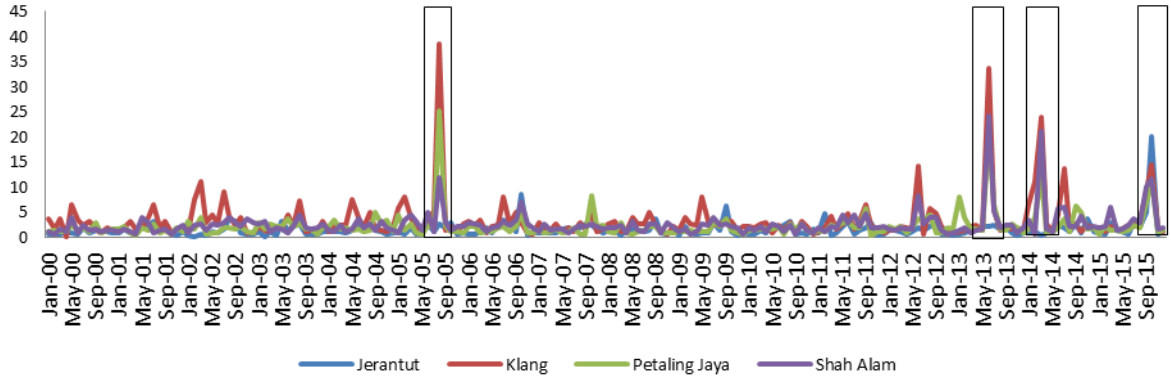

(b)

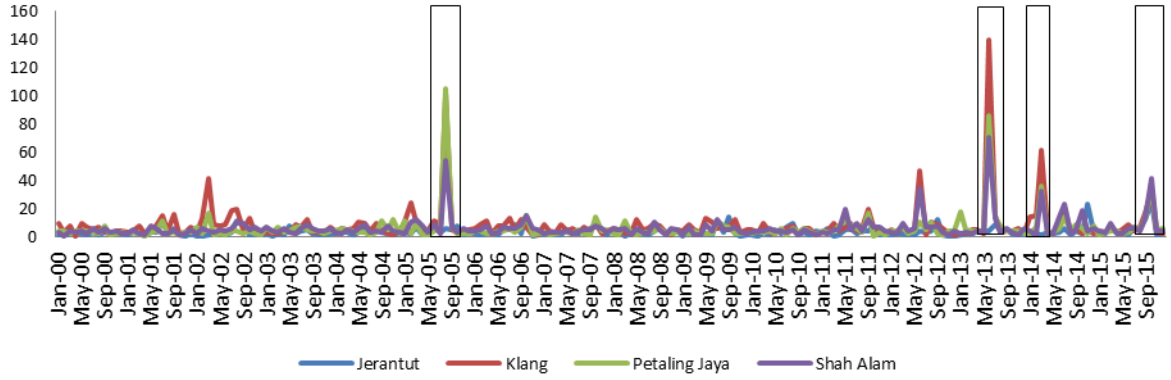

(c)

Fig. 6. (a) sum_1 of all lifetimes (b) avg_1 of all lifetimes and (c) max_1 of all lifetimes for four air quality monitoring stations Jerantut, Klang, Petaling Jaya and Shah Alam.

518